

Characterization of Native and Recombinant Bone Sialoprotein: Delineation of the Mineral-Binding and Cell Adhesion Domains and Structural Analysis of the RGD Domain*

JOHN T. STUBBS III,¹ KEITH P. MINTZ,^{1,2} EDWARD D. EANES,¹ DENNIS A. TORCHIA,¹
and LARRY W. FISHER¹

ABSTRACT

Bone sialoprotein is a small, sulfated, and phosphorylated integrin-binding glycoprotein apparently found only in tissues that eventually mineralize. Nondenatured bone sialoprotein (BSP) purified from rat osteosarcoma cell line (UMR 106-01 BSP) culture media is shown to have a hydroxyapatite $K_d \approx 2.6 \times 10^{-9}$ M, perhaps the strongest affinity for this mineral of any of the matrix proteins. Both native BSP and a 47 kD fragment of UMR-BSP (Fragment 1 ~133A~265Y) are more potent inhibitors of seeded hydroxyapatite crystal growth than recombinant human BSP fragments lacking post-translational modifications. The recombinant proteins, however, do show reproducible inhibitory activity, suggesting that at least some of the strong mineral-binding properties are encoded directly within the protein sequence itself. BSP facilitates the adhesion of several cell types through its integrin binding (RGD) tripeptide sequence. Nuclear magnetic resonance (NMR) analysis of a ¹⁵N-enriched 59 amino acid recombinant domain containing the RGD tripeptide shows that the structure of this isolated domain is highly flexible with or without 5 mM calcium. Previous work has also shown that an endogenous fragment of UMR-BSP (Fragment 1) supports cell adhesion in the absence of the RGD sequence. In this report, non-RGD cell adhesion sites are localized within conserved amino- and carboxy-terminal tyrosine-rich domains of recombinant human BSP. Given the proximity of the latter non-RGD cell adhesion site to the RGD tripeptide, a model of BSP-receptor interactions is presented. (J Bone Miner Res 1997;12:1210-1222)

INTRODUCTION

BONE SIALOPROTEIN (BSP) is a sulfated and phosphorylated glycoprotein that has been found in the mineralized matrix of bones and teeth. Subsequent work has shown that BSP is produced by osteoblasts, developing osteocytes,

osteoclasts, hypertrophic chondrocytes, odontoblasts, and cementoblasts.⁽¹⁻⁴⁾ There are two sites outside the skeleton where BSP has been reported: placental trophoblasts⁽²⁾ and certain breast carcinomas.⁽⁵⁾ Like the tissues in the skeleton, placental trophoblasts and breast carcinomas are observed to form hydroxyapatite (HA) nodules with time. Interestingly, preliminary results from a retrospective study suggest that breast carcinomas, which express large amounts of BSP, were more likely to be the subclass that had an increased propensity to metastasize to bone.⁽⁶⁾

BSP has long been hypothesized to be directly involved

*Presented in abstract form at The American Society for Bone and Mineral Research Annual Meeting, Baltimore, MD, U.S.A., September 1995.

¹Craniofacial and Skeletal Diseases Branch, National Institute of Dental Research, National Institutes of Health, Bethesda, Maryland, U.S.A.

²University of Vermont, College of Medicine and College of Agriculture and Life Sciences, Department of Microbiology and Molecular Genetics, Burlington, Vermont, U.S.A.

TABLE 1. DNA OLIGOS USED IN THE CONSTRUCTION OF RECOMBINANT HUMAN BSP

LF-135	5-gcagccggatcctcactcactttctcatagattcatatc-3
LF-136	5-ggcagccatattgcaatccagcttccaagaag-3
LF-130	5-ggcagccatattgcaatcaggggagtagc-3
LF-131	5-gcagccggatcctcactggtggtggtggtgatt-3
LF-132	5-aacggggaacctaagcggagaattaccga-3
LF-133	5-tcggtattctccgcttaggttccccgtt-3
JS-2	5-ggcagccatattgcaagtgatgaaacgaac-3
JS-3	5-ggcagccatattgctgctcactggagccaatgc-3
JS-4'	5-gcagccggatcctcaccctcctggtgggaagtg-3
LF-220	5-taattcgatccgcgattttccagttcaggca-3
LF-221	5-gtgggtcctcgagctcttttagctttgtttgtt-3

with the mineralization process. In fact, BSP protein and mRNA levels are strongly up-regulated concurrent with the mineralization process in vitro,^(7,8) and preliminary evidence suggests that null mutants of the mouse *ibsp* gene exhibit some skeletal and tooth abnormalities.⁽⁹⁾ Studies conducted by Bianco and coworkers have shown that at least a portion of the BSP secreted by rat osteoblasts is associated with electron-dense aggregates that correspond to sites of the earliest bone mineral formation.⁽¹⁰⁾ Moreover, Hunter and Goldberg have shown that BSP isolated from bone could initiate hydroxyapatite formation in an agarose gel system⁽¹¹⁾ and that chemically treating the BSP with a reagent that modified carboxylic acid groups appeared to destroy this activity.⁽¹²⁾

BSP facilitates cell adhesion of several cell types including fibroblasts, osteoclasts, chondrocytes, osteoblasts, and breast tumor cells.^(13–18) Upon sequencing the rat BSP cDNA, Oldberg and coworkers first deduced that this protein contained the integrin-binding (RGD) tripeptide⁽¹⁹⁾ and showed that BSP could support cell attachment in vitro through an integrin likely to have been the vitronectin receptor.⁽²⁰⁾ Subsequent sequencing of human, pig, mouse, hamster, and chicken^(21–25) BSP cDNAs have all shown a number of conserved domains, including the RGD tripeptide. Recently, Mintz and coworkers reported the existence of an RGD-independent cell adhesion sequence within a 47 kD fragment (Fragment 1) isolated from osteosarcoma cells.⁽¹⁶⁾ Preliminary studies with recombinant human BSP confirmed the existence of RGD-independent cell attachment site(s).⁽²⁶⁾

Traditionally, BSP has been isolated from the mineralized compartment of young bone using denaturing conditions. We utilized rat BSP isolated from the culture media of an osteosarcoma cell line under nondenaturing conditions^(16,27) and recombinant human BSP isolated from *Escherichia coli* to explore (1) the property of BSP to modulate hydroxyapatite growth and (2) the property of BSP to facilitate cell adhesion via its interaction with cell surface molecules. In this report, we directly test the hypothesis that the “polyglutamic acid” domains of human BSP contribute to the ability of this highly post-translationally modified protein to bind to hydroxyapatite and to inhibit seeded hydroxyapatite crystal growth. Moreover, we utilized recombinant human BSP to iden-

tify domains that are critical for RGD-independent cell surface protein interactions.

MATERIALS AND METHODS

Nondenatured BSP and Fragment 1

Intact rat BSP protein (amino acids 17F–320Q) and a defined fragment, Fragment 1 (amino acids ~133A–~281Y), were purified from the medium of rat osteosarcoma UMR 106-01 BSP cells using nondenaturing conditions as previously described.^(16,27)

Polymerase chain reaction generation of LysAlaGlu mutant BSP sequence from human RGD (ArgGlyAsp) BSP sequence

Synthetic DNA oligo primers complementary to the human cDNA RGD tripeptide encoding region were generated to alter the RGD-encoding DNA sequence to LysAlaGlu (KAE) in a three-step polymerase chain reaction (PCR). In the first reaction, a *NdeI*-containing sense primer complementary to the 5' end of the human BSP RGD domain and an antisense primer encoding a mutated KAE were used to amplify a product that contained *NdeI* and KAE-encoding sequences. In a second reaction, a *BamHI*-containing antisense primer complementary to the 3' end of the human BSP RGD domain and a sense primer encoding a mutated KAE were used to PCR amplify a product that contained *BamHI* and KAE-encoding sequences. The products of the first and the second PCR reactions were isolated and used as templates in the third PCR reaction to extend the 3' ends beyond the KAE encoding region, thus generating a full-length mutant human KAE domain that contained a 5' *NdeI* site and a 3' *BamHI* site. This PCR product encoding the mutated human BSP KAE region was isolated and digested with *NdeI* and *BamHI* restriction endonucleases. The presence of the KAE mutation was confirmed by DNA sequencing (data not shown).

Production of recombinant proteins

Recombinant human BSP fragments were made in *E. coli* BL-21 (DE3) cells using either the pET-15b or pET-22b vectors, purchased from Novagen. Inserts were made by routine PCRs using sequence-specific oligonucleotides (Table 1), Taq polymerase (Perkin Elmer Corp., Norwalk, CT, U.S.A.) and the human BSP cDNA plasmid, B6-5g,⁽²¹⁾ as template. The sequences encoding the in-frame restriction sites for *NdeI* and *BamHI* for pET-15b, and *BamHI* with *XhoI* for pET-22b were added via the oligonucleotides. Stop codons were added to the 3' end of each pET-15b construct to end the fusion protein with the stated amino acid. PCR products were gel purified, restriction enzyme digested, and ligated into appropriately prepared vector DNA. Competent cells were transfected and selected for plasmid incorporation on ampicillin plates. Five to ten colonies were picked, grown in liquid LB-ampicillin broth, and treated with 1 mM (final) IPTG (isopropyl- β -D-thiogalactopyranoside, Boehringer Mannheim GmbH, Mannheim,

Germany) to determine which of the selected colonies would express the recombinant protein as determined by sodium dodecyl sulfide polyacrylamide gel electrophoresis (SDS-PAGE). In each case, we first attempted to make a fragment in the pET-15b vector for expression in the cytosol of the bacterium. For fragment 57R–258E, however, the pET-15b construct was not efficiently made and it was re-engineered for expression using the short fusion propeptide that directs the synthesis to the pericellular environment using the pET-22b vector. Both vector systems include a His₆ fusion peptide that allowed purification on a the Novagen nickel-affinity resin, His-Bind. After determining which colonies supported successful production of their respective recombinant fragments, each was grown in 1 l batches in LB broth containing ampicillin and induced to produce the recombinant protein by addition of IPTG when the A₆₀₀ was 0.8–1.0. The cells were harvested after 1–2 h of induction. In two cases, 17F–146E and 57R–258E, the recombinant fragments were insoluble in the Novagen's recommended nondenaturing extraction buffer and required the addition of 6 M urea prior to purification on the column. Each protein was purified on 5 ml His-Bind columns using Novagen protocols (denaturing or nondenaturing conditions as required) with the exception of fragment 205S–281E which was eluted from the column in 150 mM imidazole rather than the suggested 1 M imidazole. The recombinant human osteopontin fragment 173K–314N was made in the pET-15b vector using the same approach and the OP-10 plasmid as template.⁽²⁸⁾ Whenever the purity of a protein was insufficient as determined by SDS-PAGE, a second (0.5 ml) His-Bind column was used. Eluted recombinant proteins were dialyzed (3.5 kD molecular weight cut-off) exhaustively against water and lyophilized. All proteins were judged to be ~95% pure by SDS-PAGE analysis and the mass of selective recombinant proteins was verified by matrix assisted laser desorption ionization time of flight mass spectrometry (MALDI-TOF) (Ref. 29 and data not shown). Lyophilized dry weight was used to determine protein concentrations in all subsequent experiments unless stated otherwise.

Production of ¹⁵N-enriched recombinant RGD domain of BSP

The RGD domain of human BSP (258E–317Q) was prepared under nondenaturing conditions as above except that the bacteria were grown in M9 minimum media containing [¹⁵N]NH₄Cl (Cambridge Isotope Laboratory) as the sole nitrogen source and supplemented with 50 µg/ml ampicillin, 1 mM thiamine, 2 mM MgSO₄, and 0.1 mM CaCl₂. The pET-15b fusion peptide was removed from the purified protein by digestion overnight at room temperature with human thrombin (Novagen) according to the manufacturer's recommended procedures, passed through a 50 kD Filtron Macrosep ultrafiltration membrane to remove the thrombin-related proteins, and then loaded onto a fresh His-Bind column. Although lacking the His₆ fusion peptide, the RGD domain bound to the column in 5 mM imidazole loading buffer, was retained in the wash buffer (60 mM imidazole) and eluted in 150 mM imidazole, all in 0.5 M

NaCl, 0.02 M Tris, pH 7.9. The purified protein was then dialyzed against water and concentrated to ~10 mg/ml (determined via UV absorbance) on a 1 kD cut-off Filtron Microsep centrifugal concentrator at 4°C. According to Novagen, the thrombin treatment leaves a 4 amino acid fusion peptide, GSHM, attached to the amino terminus of the recombinant protein.

Apatite seed crystal preparation

The hydroxyapatite HA seed crystals used in the experiments were prepared by adding, with stirring, 50 ml of an unbuffered 0.1 M CaCl₂ solution adjusted to pH 7.4 into 50 ml of a 0.1 M HEPES-buffered, pH 7.4, 0.01 M NaN₃ stabilized, 0.06 M KH₂PO₄ solution. The precipitated slurry (which formed immediately upon mixing) was kept at pH 7.4 with 1.0 M NaOH by means of a pH-Stat (Metrohm Combitorator 3D, Brinkmann Instruments) until base was no longer required (28 h), then adjusted to 300 mmol/kg in osmolality with solid NaCl, and stored at room temperature until use. The apatitic nature of the seed material was confirmed by X-ray diffraction (data not shown).

Determination of BSP-hydroxyapatite dissociation constant

BSP was metabolically labeled with [³H]glucosamine and [³⁵S]sulfate and purified as previously described.⁽³⁰⁾ The binding of BSP to hydroxyapatite crystals was determined by competition of metabolically labeled BSP with unlabeled BSP on 10 µg of hydroxyapatite crystals (0.00153 m² of crystal area). All dilutions of the protein and crystals were made in seed crystal buffer after the matured crystals were removed by centrifugation. HA crystals were incubated with a constant amount of labeled BSP with increasing amounts of unlabeled BSP for 30 minutes at 20°C and constant shaking. Following the incubation period, the crystals were removed from the aqueous phase by centrifugation at 12,000g for 10 minutes. The supernatants were carefully removed and the radioactivity in the unbound fractions was determined by scintillation spectroscopy. The pellets were dissolved in 0.1 ml of 0.5 M EDTA, pH 6.0, and the bound radioactivity was also measured. The dissociation constant was determined using a modified Scatchard analysis.^(31–33)

Hydroxyapatite seed growth inhibition

Lyophilized protein samples were dissolved to concentrations of 10–20 µM in 0.05 M HEPES (pH 7.5) adjusted to 300 mmol/kg in osmolality with NaCl. Solutions were stored at 5°C until use. Seeded reaction slurries (2.0 ml total volume) were prepared in 5.0 ml polystyrene vials by sequentially adding to the appropriate volume of 0.05 M HEPES solution, 0.667 ml of 0.0045 M Ca(NO₃)₂ in 0.05 M HEPES, 0.04 ml of 0.05 M KH₂PO₄ in 0.05 M PIPES, the appropriate volume of protein solution, and 0.022 ml of the seed slurry (4.6 mg/ml). All solutions were adjusted to pH 7.5 and to 300 mmol/kg in osmolality with NaCl before use. Starting Ca, PO₄, and protein concentrations were 1.5, 1.0, and 0.0005 mM, respectively. Initial seed concentration was

0.05 mg/ml. Once mixed, the vials were sealed and agitated continuously on a Clay-Adams Nutator at room temperature (22°C). At appropriate intervals, 0.5 ml aliquots were expressed through 0.22 μm pore Millex-GS filter units (Millipore Corp., Bedford, MA, U.S.A.), and the filtrates were analyzed for Ca^{2+} by atomic absorption spectrometry (Model 603, Perkin Elmer). The filtrate Ca^{2+} values were not corrected for protein binding. At 0.5 μM , insufficient protein was present in the reaction solution to bind more than negligible amounts of Ca^{2+} (<0.02 mM compared with the starting 1.5 mM Ca^{2+}).

Preparation of coated bacteriological plates for adhesion assay

A modification of the cell adhesion assay described by Mintz and colleagues⁽¹⁶⁾ was utilized to test the adhesive properties of the recombinant proteins. Briefly, 10 μl of a 55 μM recombinant human BSP protein solution (50 mM Tris-HCl pH 7.8, 110 mM NaCl) was applied in replicate to bacteriological plates (Falcon 1008, 35 \times 10 mm) and stored in a humidified environment overnight at 4°C. Each 35 mm plate received 15–24 individual dots of protein solution. Coated protein dots were aspirated the following morning and covered with 60% methanol for 2 h. Next, the methanol solution was aspirated and the entire plastic surface was coated with a blocking solution (1.0% bovine serum albumin [BSA]; 5.0 mM CaCl_2 ; 0.1 mM phenylmethylsulfonyl fluoride in 50 mM Tris-HCl, pH 7.8, 110 mM NaCl) for 1 h. This solution was aspirated at the end of 1 h and the plate was washed three times with serum-free Dulbecco's modified essential medium (DMEM) supplemented with 2.0 mM glutamine, 100 U/ml penicillin, 50 $\mu\text{g}/\text{ml}$ streptomycin, and 50 $\mu\text{g}/\text{ml}$ ascorbic acid. Sterile techniques were used throughout.

Culture and preparation of cells for BSP-cell surface protein-protein interaction assay

Confluent MC3T3-E1 mouse osteoblastic cultures were washed with three 25 ml volumes of Hank's balanced salt solution (HBSS) and trypsinized with 1 \times GIBCO (Grand Island, NY, U.S.A.) Trypsin-EDTA (0.05% trypsin, 0.53 mM EDTA) in HBSS for 15 minutes. Trypsin activity was inhibited upon the addition of heat-inactivated fetal calf serum (FCS; GIBCO) at a final concentration of 10%. Cells were allowed to recover from trypsin treatment for 2 h in the presence of 10% FCS. Next, cells were pelleted by centrifugation and washed with serum-free DMEM three times to assure the removal of FCS. The resulting cell concentration was determined with the use of a Coulter Counter.

BSP-cell surface protein interaction assay

Washed cells were agitated upon a Clay Adams Nutator in the presence or absence of 400 μM GRGDS (Calbiochem, La Jolla, CA, U.S.A.) in serum-free DMEM for 30 minutes at 37°C, 8% CO_2 . Next, approximately 30,000 cells/ mm^2 were added to the precoated bacteriological plates,

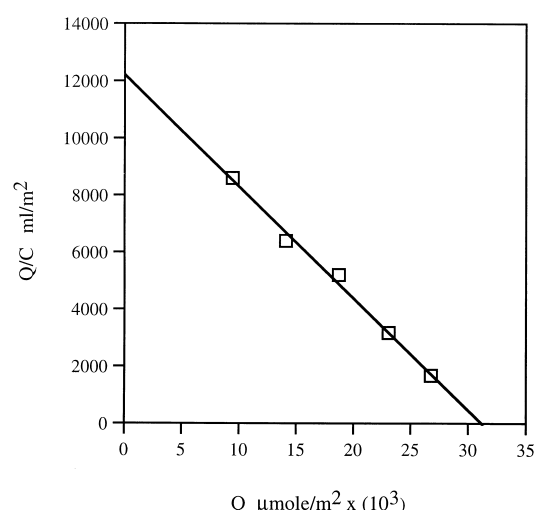


FIG. 1. An adaptation of the Scatchard plot for the binding of nondenatured UMR BSP to hydroxyapatite. The ratio of bound BSP ($Q = \mu\text{mol}/\text{m}^2$ hydroxyapatite) to unbound BSP ($C = \mu\text{mol}/\text{ml}$) is shown as a function of bound BSP. Analysis yields a dissociation constant of $\sim 2.6 \times 10^{-9}$ M.

and the cells were allowed to adhere at 37°C, 8% CO_2 overnight. Nonadherent cells and tissue culture media were aspirated from the culture the following morning. The plates were washed with 3 vol of serum-free DMEM, covered with 80% methanol, and refrigerated at -20°C for 20 minutes to fix adherent cells. Nuclei of adherent cells were stained with a 0.1% crystal violet solution for 10 minutes. Representative fields of triplicate experiments were photographed.

^{15}N HSQC NMR⁷ analysis of the recombinant RGD BSP domain

A heteronuclear single quantum correlation (HSQC) two-dimensional nuclear magnetic resonance (NMR) spectrum of the ^{15}N isotopically labeled recombinant human RGD domain (~ 10 mg/ml in 95% $\text{H}_2\text{O}/5\%$ D_2O , pH 6) was run on a Bruker AM 500 NMR spectrophotometer set at 500 MHz ^1H frequency. The analysis was performed at 34°C in the presence and absence of 5 mM CaCl_2 .

RESULTS

BSP has long been known to have an affinity for hydroxyapatite. A UMR-BSP hydroxyapatite dissociation constant of 2.6×10^{-9} M was calculated (Fig. 1) utilizing a molecular weight of 67.9 kD and a modification of the Scatchard method.^(31–33) Plotting the same data using the Langmuir-type model⁽³³⁾ resulted in virtually the same estimation, 2.6×10^{-9} M (plot not shown).

Fully modified BSP contains phosphate, sulfate, and sialic acid groups and binds with high affinity to hydroxyapatite (HA). To test whether or not domains of the un-

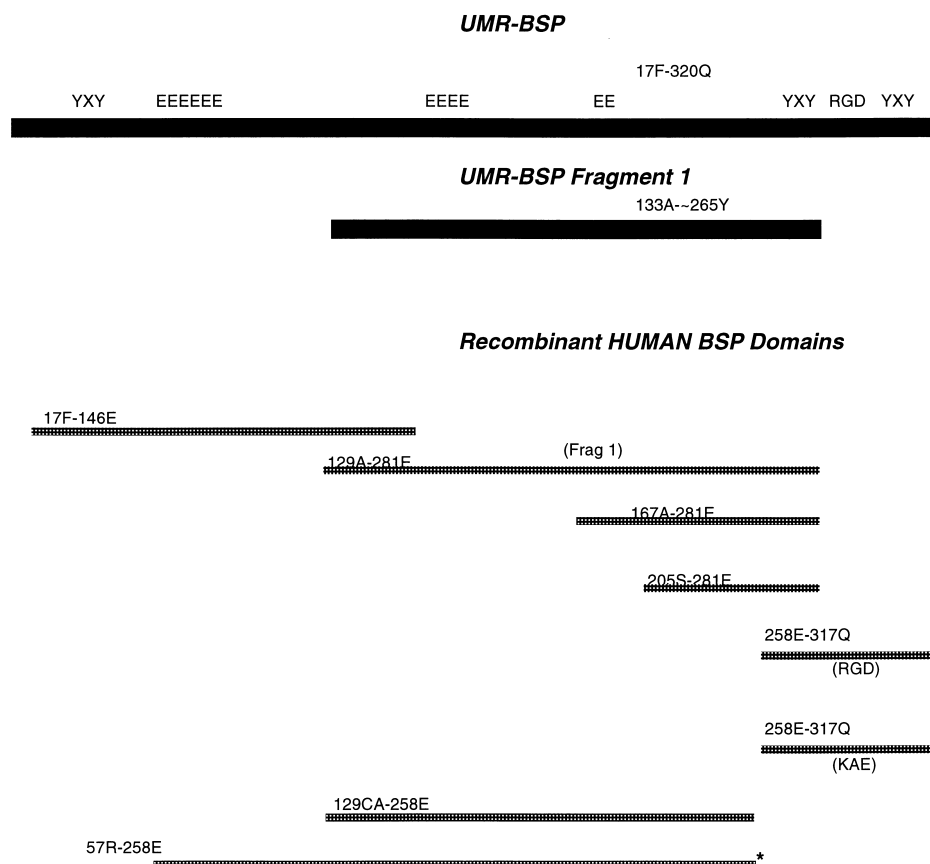


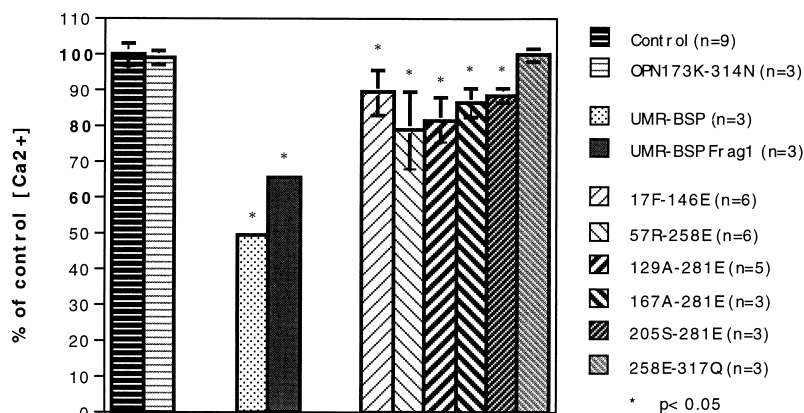
FIG. 2. Major domains of BSP with the corresponding rat UMR and recombinant human fragments used in this study. Numbers and letters on rat UMR BSP (solid lines) and recombinant human BSP fragments (stippled lines) represent their start and end point amino acids relative to full-length protein. The amino acid sequence of the rat UMR-BSP protein is larger than the corresponding human BSP protein, thus the amino acids do not align perfectly. The clustered E's represent the "polyglutamic acid" regions; the Y's, the tyrosine-rich regions; and RGD, the integrin-binding tripeptide. (The rat RGD domain is located at 289–291, while the human RGD domain is located at 286–288.)

derlying protein sequence may be contributing to the HA binding, we produced a series of overlapping recombinant human BSP fragments in *E. coli* (Fig. 2). (Curiously, we were unable to produce full-length BSP in the pET vector and in other vector systems.) All of the recombinant fragments had calculated isoelectric points that were acidic and all were a cyan color when stained with StainsAll (data not shown). Most proteins, including many whose isoelectric points are acidic, e.g., serum albumin, $pI = 5.7$, stain a light-sensitive pale pink with this stain while phosphoproteins and proteoglycans stain a light-stable blue/purple.⁽³⁴⁾ This suggests that spacing of the acidic groups within these modification-free recombinant proteins results in metachromasia of the StainsAll dye usually associated with post-translationally modified proteins. (A recombinant fragment of human osteopontin that contains the aspartic acid-rich domains also stains cyan with StainsAll; L. Fisher, unpublished data.) Interestingly, all of these acidic fragments electrophoresed as bands of higher molecular weight than predicted by sequence alone. (Mass spectral analysis of selected recombinant BSP proteins also confirmed this observation; data not shown). Aberrant migration has been

reported for recombinant osteopontin, a protein that shares similarities with BSP in that it is rich in acidic amino acids.⁽³⁵⁾ This suggests that at least some of the electrophoretic mobility aberrancy observed for BSP is likely due not just to post-translational modification but also to the acidic domains themselves.

One of the commonly held tenets of mineral nucleation by proteins is that a nucleating protein is fixed to a solid phase by one portion of its sequence while another domain binds the ions in an appropriate orientation to create a pseudocrystal lattice. Subsequent ions accumulate on this high affinity surface and, with time, a self-sustaining crystal is formed and grows. One corollary of this hypothesis is that the domain that contains the direct nucleation site should, when not fixed to a solid support, have sufficient affinity for the same crystals in solution to poison their growth in a metastable solution. We have used this property of the soluble form of a putative nucleator to inhibit the growth of crystal to ascertain if the acid domains of BSP, free of post-translational modifications, may be candidates for nucleating HA crystals. In a previous study, we had rapidly screened all of the fragments simply for the ability to bind

FIG. 3. Inhibition of hydroxyapatite seeded crystal growth by UMR BSP, Fragment 1, and various recombinant human BSP fragments. Excess hydroxyapatite seed crystals were allowed to grow for 6 h at room temperature in a metastable solution of Ca^{2+} and PO_4 either in the absence (control) or presence of $0.5 \mu\text{M}$ protein. Loss of Ca^{2+} from the solution is shown as the mean percent of control \pm SD. The number of samples are indicated by n . Values of $*p < 0.05$ are relative to the control and are based upon a two-tailed Dunnett's test.



to HA as measured by the loss of the protein from a solution that contained an excess of HA crystals. All of the fragments bound to the crystals and were removed from the supernatant.⁽²⁹⁾ In this study, the purified proteins were added to an excess of HA seed crystals suspended in a supersaturated solution of calcium and phosphate. The control tubes, which contained no protein, lost free Ca^{2+} to the growing crystals at an unimpeded rate. Other tubes contained equimolar amounts of either (1) the natural UMR-derived BSP, (2) the large UMR degradation product, Fragment 1, or (3) one of the recombinant human BSP fragments. If a protein bound to the growing HA crystals in a way that hindered crystal growth, the loss of Ca^{2+} in the supernatant would be at a decreased rate. The loss of Ca^{2+} was determined as measured by atomic absorption. These data are expressed in Fig. 3 as the percent of control where a value less than 100% represents a slower loss of calcium ion from the solution due to poisoning of the HA crystal growth by the added protein. The data shown are after 6 h of growth, but essentially the same results were seen for 3 h and 24 h time points also. While each protein could have been added in sufficient amounts to inhibit completely the crystal growth, we used equimolar amounts of proteins with the most potent inhibitor being limited to a maximum of ~50% inhibition. This allows for a direct, equimolar comparison of the various proteins.

The two proteins with the strongest molar inhibition of the crystal growth, intact BSP and Fragment 1, were the two that were obtained from eucaryotic cell culture media and therefore contained acidic post-translational modifications including sialic acid, oligosaccharides, sulfate groups, and presumably phosphate groups. All of the recombinant fragments that contained one or more of the three "polyglutamic acid" domains were able to suppress crystal growth, but none were as potent as the post-translationally modified products. In addition, two fragments that were acidic but lacked any of the "polyglutamic acid" stretches (205S-281E and 258E-317Q) also inhibited hydroxyapatite growth but were significantly less active on a molar basis than the "polyglutamic acid" containing recombinant BSP proteins. A fragment of recombinant human osteopontin (173K-314N), the carboxy-terminal half that lacks the "polyaspartic acid" domains, is an example of an acidic (pI = 4.8)

protein with no significant ability to inhibit seeded crystal growth. Note, the inactivity of this protein also demonstrates that the fusion peptide does not contribute to hydroxyapatite inhibitory activity.

BSP facilitates the adhesion of several cell types through its RGD sequence. The BSP carboxy-terminal domain includes the RGD integrin-attachment tripeptide and the sites of tyrosine sulfation but none of the many carbohydrate chains found in the other domains of the native molecule. A 59 amino acid recombinant RGD domain was produced in minimal media using $^{15}\text{NH}_4\text{Cl}$ as the sole source of nutrient nitrogen. The HSQC two-dimensional NMR spectrum showed a narrow spread of chemical shifts (Fig. 4) characteristic of a flexible structure or "random coil." This spectrum was the same with 5 mM Ca^{2+} .

BSP also facilitates cell adhesion through non-RGD sequences. Mintz and coworkers observed cell adhesive activity within an enzymatically clipped form of UMR-BSP, Fragment 1, that lacked the RGD cell attachment sequence.⁽¹⁶⁾ The observed cell attachment event was due to an interaction between a cell surface protein and either a post-translational ligand or the underlining protein sequence. The recombinant human version of UMR-BSP Fragment 1 (129A-281E) expressed in *E. coli* was tested for its ability to facilitate cell attachment of mouse MC3T3-E1 osteoblasts. This and all of the attachment experiments were performed by dotting $10 \mu\text{l}$ portions of equimolar concentrations of various proteins in replicate dots on a single 35 mm dish. Positive and negative controls were included in the experiments. A single dilution of cells (plus or minus competing peptides) was then exposed to the multiple dots simultaneously under identical conditions. The replicate dots were stained with crystal violet and scored for the presence or absence of attachment. The Fragment 1 recombinant protein facilitated cell attachment (Fig. 5A), thus suggesting that the attachment activity of the original UMR-Fragment 1 is due at least to a significant degree to the underlying protein sequence. Attachment to the recombinant protein was not blocked by the addition of GRGDS peptide (Fig. 5D). Inspection of the BSP Fragment 1 protein sequence had revealed a potential cell attachment domain at the N terminus that is homologous to the fibrinogen γ chain, KQAGD.⁽³⁶⁾ Several BSP deletion

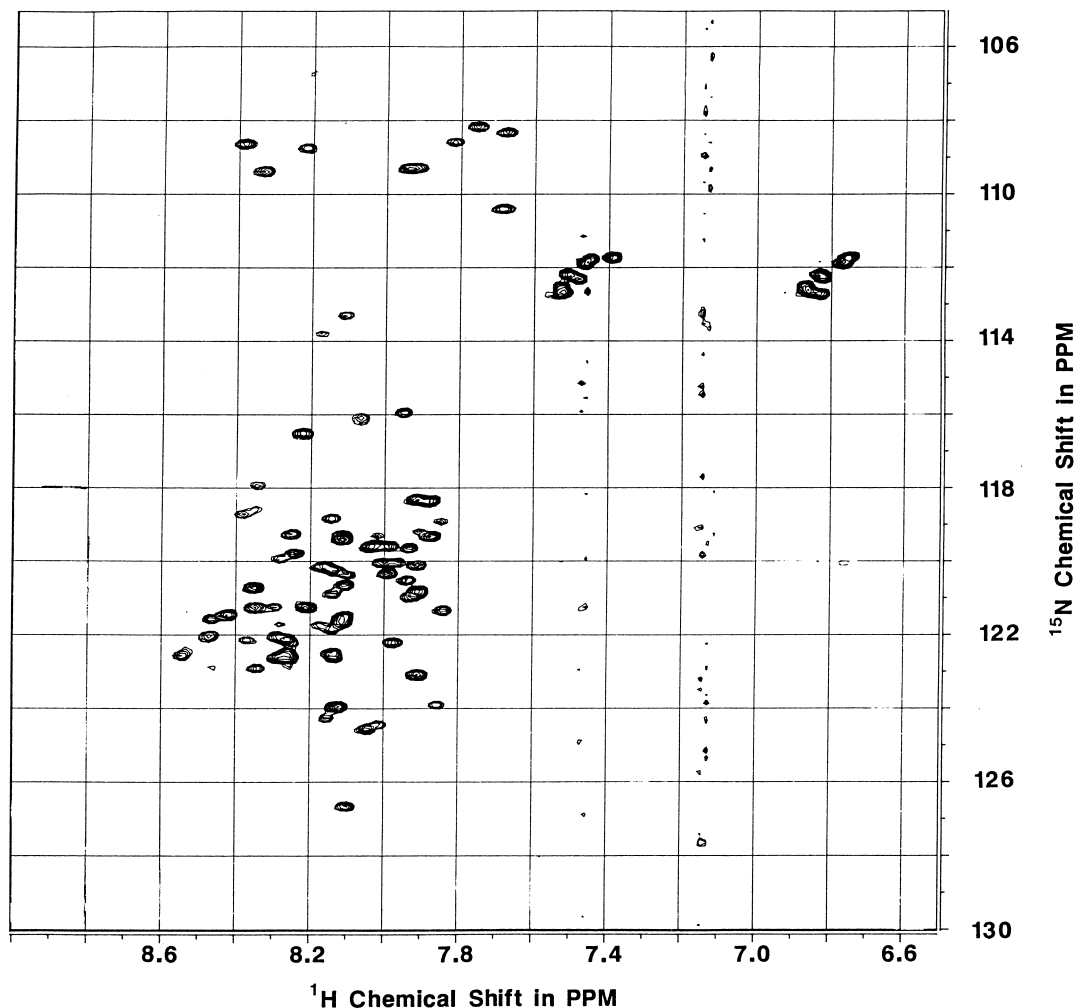


FIG. 4. HSQC two-dimensional NMR spectrum using ^{15}N -labeled recombinant human protein 258E-317Q, the RGD domain of BSP. The narrowness of the spread of backbone chemical shifts of only 7.6–8.6 parts per million (PPM) is indicative of a rapidly flexing protein, i.e., a “random coil.” The strength of the peaks suggests that the protein remains monomeric at ~ 10 mg/ml.

proteins that spanned the length of Fragment 1 were generated and tested to localize the cell attachment region. The smallest protein that facilitated cell attachment was not the fibrinogen-like domain but a C-terminal protein 205S-281E (Fig. 5B). Furthermore, protein C129A-258E that lacked C-terminal sequences present in 205S-281E failed to promote cell attachment under our conditions (Fig. 5C). This suggests that the interactions between BSP-UMR Fragment 1 and the cells were mediated by tyrosine-rich sequences 258E-281E.

This result was also confirmed using a small recombinant protein containing this tyrosine-rich area as the amino terminus in which all three amino acids, RGD, were mutated to KAE, thus negating the contribution of integrin-binding RGD tripeptide to cell attachment. Mutation of the RGD arginine to lysine or glycine to alanine has been reported to result in a reduction of adhesion activity while mutation of the RGD aspartic acid residue has been reported to abolish cell adhesion activity.⁽³⁷⁾ As was the case for all other

recombinant proteins that contained the tyrosine-rich domain, 258E-317Q (KAE) did support attachment of MC3T3-E1 cells (Fig. 6B). However, unlike the other recombinant BSP proteins, both the normal 258E-317Q (RGD) protein and the mutant 258E-317Q (KAE) protein-mediated cell attachment were affected by the addition of GRGDS peptide (Figs. 6D and 6E).

The conserved tyrosine-rich domain found near the amino terminus of the BSP protein was also tested for cell attachment activity. Using the same recombinant technology, we produced a series of proteins that either included or lacked this tyrosine-rich domain. Cell adhesion was observed when we utilized a protein (17F-146E) that contained the N-terminal tyrosine-rich repeat and, furthermore, this was not inhibited by GRGDS (Figs. 7A and 7B). Cell adhesion was not observed when we utilized an overlapping recombinant protein (57R-258E) that lacked the N-terminal tyrosine-rich domain (Fig. 7C). This suggests that BSP sequences 17F-57R facilitate RGD-independent

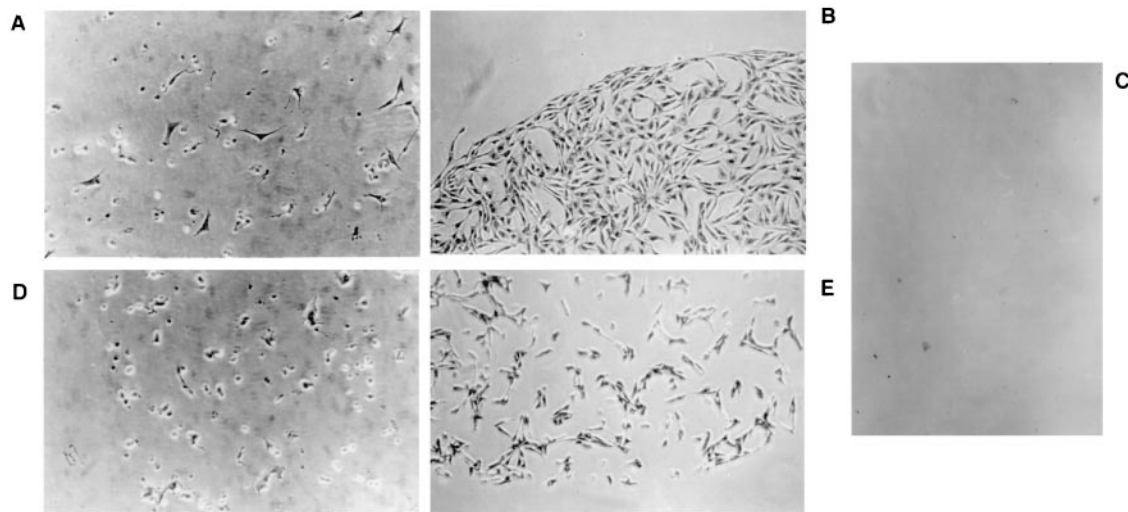


FIG. 5. Localization of a non-RGD cell attachment site within a carboxy-terminal tyrosine-rich domain of BSP. UMR-106 BSP Fragment 1 lacks a RGD sequence, yet it facilitates cell attachment.⁽¹⁶⁾ (A) Recombinant human BSP Fragment 1 (129A–281E) facilitated MC3T3-E1 cell attachment. (B) However, the smallest portion of this region to facilitate cell attachment, 205S–281E, corresponded to the carboxy-terminal end of Fragment 1. (C) A recombinant human BSP fragment that lacked carboxy-terminal sequences, C129A–258E, failed to promote cell attachment. Cellular adhesion to recombinant BSP protein (D) 129A–281E and (E) 205S–281E is resistant to 400 μ M GRGDS.

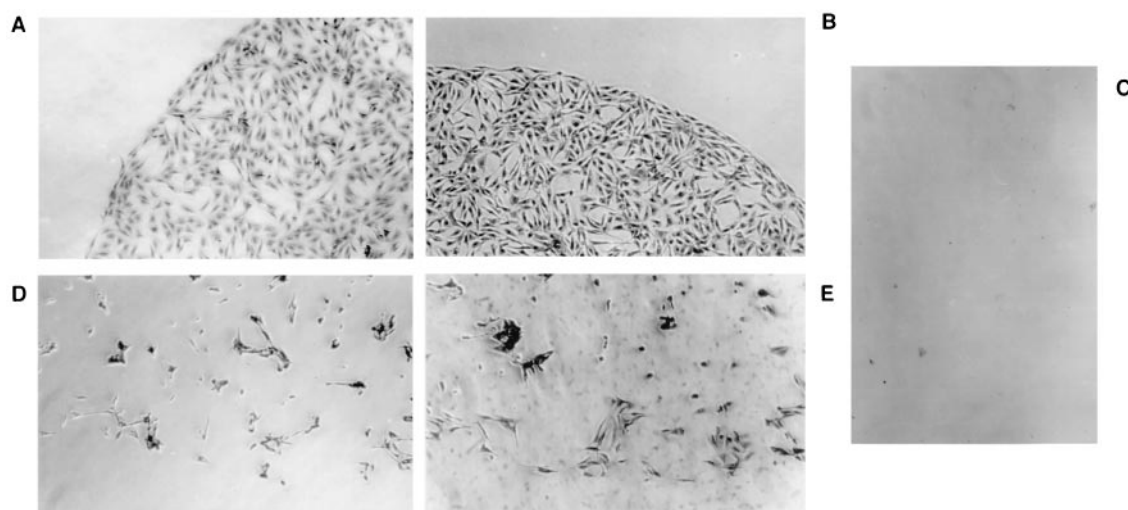


FIG. 6. Mutation of the RGD sequence to KAE does not abolish cell attachment activity of recombinant human BSP. The recombinant RGD BSP domain and a mutated KAE BSP domain (258E–317Q) were tested for MC3T3-E1 cell adhesion activity. (A) The recombinant human RGD domain facilitated cell attachment. (B) The KAE mutation also supported cell attachment. (C) The negative control, C129A–258E, failed to promote cell attachment. Note that cell adhesion mediated by the (D) RGD and (E) KAE domains is sensitive to 400 μ M GRGDS.

cell attachment. The same result was observed whether the proteins were tested on an equal mass or equal molar basis.

DISCUSSION

BSP is an extracellular matrix glycoposphosulfoprotein whose localization has generally been limited to tissues that mineralize at some point during development or pathology.

Two important properties of this interesting protein known for several years are (1) BSP has an affinity for hydroxyapatite being found at the earliest mineralization sites and (2) BSP can support cell attachment through integrins. The former property has led many to speculate that BSP may be important for the nucleation of HA in at least certain matrices, while the latter property has led to the speculation that cells positive for the vitronectin receptor may bind to extracellular matrices that contain BSP. In this paper, we

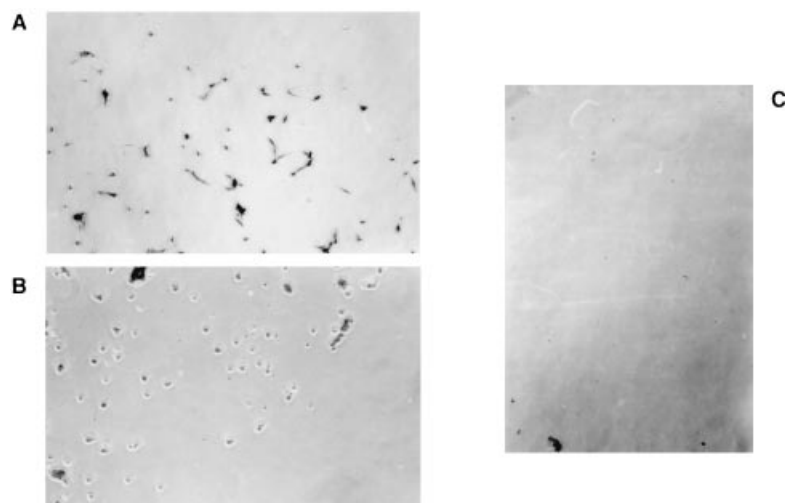


FIG. 7. Localization of a non-RGD cell attachment site in the amino-terminal tyrosine-rich domain of BSP. Two overlapping recombinant human BSP proteins that span the N terminus of BSP were tested for MC3T3-E1 cell adhesion activity. (A) Recombinant human BSP fragment 17F-146E facilitated MC3T3-E1 (B) cell attachment; however, (C) an overlapping BSP fragment 57R-258E did not. Cell adhesion mediated by the N-terminal non-RGD cell attachment site is resistant to 400 μ M GRGDS.

have explored several physicochemical and biological properties of both nondenatured BSP isolated from cell culture and several recombinant fragments isolated from *E. coli*.

The use of a modified Scatchard analysis of the binding of the UMR-derived BSP to HA crystals has resulted in a value of 2.6×10^{-9} M. This value appears to represent the strongest HA-binding yet for a matrix protein,⁽³⁸⁾ although caution should be taken when directly comparing the dissociation constants produced by different investigators using different experimental conditions. Furthermore, the relative strength of the dissociation constant between a protein and a crystal surface, once values become greater than that which causes significant binding, may not necessarily be directly relevant to the biology of the tissue.

The calculated isoelectric point of the underlying protein for both rat and human BSP is 3.9. This is sufficiently acidic to suggest that BSP should bind tightly to HA and may even be able to nucleate these crystals if bound to an appropriate matrix in the proper orientation. However, fully half of the weight of BSP is composed of acidic post-translational modifications, including phosphorylation,^(39,40) sulfation,⁽⁴¹⁾ and carbohydrate groups containing sialic acids.⁽²¹⁾ Interestingly, rabbit BSP is even more heavily modified, being a keratan sulfate proteoglycan.⁽⁴²⁾ To test if portions of the unmodified protein alone could reasonably contribute to apatite binding, we have produced a series of overlapping recombinant proteins. These unmodified proteins were tested for their relative abilities to bind to HA and to significantly alter the growth of nucleated crystals in a supersaturated solution. Our results clearly showed that while all recombinant fragments bound to HA crystals, none of them could inhibit nucleated crystal growth as well on a molar basis as either intact rat BSP or one of its major fragments, Fragment 1. This suggests that post-translational modifications either directly or indirectly contribute to the ability of BSP to bind strongly to HA crystal surfaces. Furthermore, because a number of recombinant fragments (extending over two-thirds of the molecule) were active in the crystal poisoning study, it seems unlikely that a single short stretch of the BSP protein sequence is responsible for

the majority of the HA-binding ability of BSP. This is not to say, however, that short segments of the BSP sequence do not play unique and critical roles in the complex interplay of proteins and ions that ultimately lead to biologically controlled mineralization. Nevertheless, we can state that the inhibitory effect of the recombinant proteins upon HA seeded growth is not due only to the acidic nature of the protein since two recombinant proteins (BSP 258E-317Q and OPN 173K-314N) have acidic isoelectric points yet failed to inhibit seeded crystal growth under our experimental conditions.

The observation that recombinant BSP fragments can effectively inhibit seeded HA crystal growth is necessary but not sufficient to show that the underlying protein sequence can nucleate HA crystals in vitro. Using BSP isolated from porcine bone and an agarose gel matrix, Hunter and Goldberg⁽¹¹⁾ have presented evidence that, when fully modified, this protein can nucleate HA in vitro. Furthermore, they have shown that upon reacting the BSP with a chemical that modifies all carboxylate groups, this activity is lost.⁽¹²⁾ From this elegant study, the authors suggested that the nucleation of HA by BSP involved one or more of the glutamic acid-rich domains. The modifying chemistry used in the above reference, however, will also modify the sialic acid carboxyl groups,⁽⁴³⁾ thus complicating the issue of whether the glutamic/aspartic acid modifications were the sole reason for the loss of HA-nucleating property. Our results add support to the hypothesis that the glutamic acid residues may be directly involved in the interaction of BSP with HA and therefore may be capable of nucleating HA crystals. A second complication of the chemically induced loss of nucleation experiments is that if nucleation requires that the nucleator be bound to a matrix to induce crystal growth, then a modification that changes the protein's ability to bind to the matrix may also destroy the nucleation property irrespective of changes in the actual nucleation site on the BSP. By analogy, future nucleation experiments designed to study the ability of BSP fragments to nucleate HA crystals will similarly be complicated by the probable deletion of the purported matrix-binding site in many of the constructs.

TABLE 2. (A) COMPARISON OF BSP C-TERMINAL TYROSINE-RICH REGIONS AMONG SPECIES

Human	GEYEYTGANDYDNGYEIYESE
Cow	GEYEQTGTNEYDNGYEIYESE
Pig	GEYEQTGAHEYDNGYEIYESE
Hamster	GEYEQTGNNEYNGEYQIYDNE
Rat	GEYEQI G NEYNTAYETYDEN
Mouse	GEYEQTG NEYNNEYEVDNE
Consensus	GEYE --- G ----- Y ---- Y --- Y ---

(B) COMPARISON OF BSP N-TERMINAL TYROSINE-RICH REGIONS AMONG SPECIES

Human	DSEENGVFYKYPRIYLYKHAYFYPHLKR
Cow	DSEENGVFYKYPQYYVYKHGYFYPAKR
Pig	DPEENGVFYKYPRIYLYKHAYFYPLKR
Rat	DSEENGVFYKYPRIYLYKHATYFPLKR
Hamster	DSEENGVFYKYPRIYLYKHAYFYPSLKR
Mouse	DSEENGVFYKYPRIYLYKHAYFYPLKR
Consensus	D - E - NGVFKYRP - Y -- YKH ----- P - LKR

Various mammalian cells bind to BSP.⁽¹³⁻¹⁸⁾ This adhesion event is generally regarded as an interaction between the BSP RGD tripeptide and cell surface integrins. Mintz and coworkers, however, isolated a fragment of BSP (Fragment 1) from UMR-106 osteosarcoma cells that facilitated cell adhesion even though it lacked the RGD tripeptide.⁽¹⁶⁾ That study, however, did not determine if cell adhesion was due to the underlying amino acid sequence or to eucaryotic post-translational modifications present in Fragment 1. In the present study, overlapping recombinant human BSP proteins, lacking eucaryotic post-translational modifications, were utilized to localize the RGD-independent cell attachment domain of Fragment 1 BSP to a conserved tyrosine-rich domain found in the C terminus. Cell adhesion mediated by this domain is resistant to the GRGDS peptide in a fashion similar to the cell adhesion properties observed for UMR-BSP Fragment 1. This tyrosine-rich domain is highly conserved (Table 2a) and is immediately amino-terminal to the BSP RGD sequence. We next sought additional evidence that would implicate the involvement of this conserved BSP tyrosine-rich domain in cell attachment. Previous studies report that mutation of the RGD arginine or glycine amino acid residues results in a decrease of integrin-ligand interactions while mutation of the aspartic acid residue alone resulted in a complete loss of integrin-ligand interactions.⁽³⁷⁾ In our experiment, we synthesized a recombinant BSP protein that contained the conserved tyrosine-rich domain of Fragment 1 and completely changed the RGD to KAE to abolish completely the effect of the RGD sequence on our cell attachment assays. Since the mutated KAE-BSP domain facilitated cell attachment, the conserved tyrosine-rich repeat identified in recombinant Fragment 1 is the most plausible candidate sequence to confer this activity. However, we cannot exclude the additional contribution of the conserved tyrosine-rich domain (285E-317Q) that flanks the RGD carboxyl end in the KAE-containing

fragment. Unfortunately our attempts to synthesize this recombinant BSP domain in *E. coli* have not been successful.

Another cell attachment site within the highly conserved tyrosine-rich domain close to the amino terminus of BSP (Table 2b) was also discovered. Interestingly, the C-terminal tyrosine-rich domain can be modified by sulfation while the N-terminal tyrosine-rich domain cannot.⁽²¹⁾ *E. coli* lacks the mammalian enzyme tyrosylprotein sulfotransferase required to modify these sequences, thus attempts to compare sulfated versus nonsulfated species were not possible. Also, attempts to utilize the N-terminal tyrosine-rich domains in cell attachment competition experiments with the C-terminal tyrosine-rich domain and vice versa were unsuccessful due to the insolubility of these proteins even at μ M concentrations (GRGDS is used at 400 μ M).

Our results have shown that two independent tyrosine-rich domains of BSP, one in the amino terminus and the second in the carboxyl terminus, can support attachment in a GRGDS-resistant manner. Because of the close proximity of the carboxy-terminal cell attachment domain to the RGD sequence, it is possible that this tyrosine-rich region may bind to a portion of one or more integrins near the RGD-binding pocket (Fig. 8). This is further supported by the observation that an ~ 60 amino acid recombinant polypeptide containing this tyrosine-rich domain as its amino terminus (with the normal RGD sequence changed to the inactive, KAE) not only supports cell attachment but is subject to competition by GRGDS. Figure 8 illustrates one possibility of how the tyrosine-rich domain, when it is the carboxyl terminus, may fit into the integrin pocket even with the GRGDS peptide in place. When this domain is immediately followed by the inactive KAE region (Fig. 8), the KAE domain and the GRGDS peptide compete for the same space in the binding pocket. Because the RGD tripeptide is strongly bound in the pocket, the GRGDS peptide can first displace the nonbinding KAE region which then may disrupt the binding of the contiguous tyrosine-rich domain. With the tyrosine-rich domain displaced, this recombinant fragment can no longer support cell attachment. Alternatively, the tyrosine-rich domains may bind to a cell surface protein that is different from the RGD-binding integrin family. The effect of the GRGDS peptide may be a downstream response of living cells to the biologically active pentapeptide. To distinguish which of these models (or a combination of these models) is correct, we will, in future studies, isolate and identify the specific cell surface protein(s) binding to the various BSP fragments.

The structures of proteins are usually determined by either X-ray diffraction or NMR. The structure of BSP is unlikely to be solved by X-ray diffraction due to the difficulty of getting useful protein crystals from a molecule that contains so many carbohydrate groups. Solving structures by NMR is currently limited to highly soluble proteins with a mass of no more than about 20 kD. To overcome this difficulty, we produced an ^{15}N -enriched 59 amino acid recombinant protein corresponding to the integrin-binding carboxyl terminus of human BSP, a domain that is thought to be free of carbohydrate groups in vivo. The structure was shown to be a highly flexible and mobile chain. While this result was not surprising given the computer-generated sec-

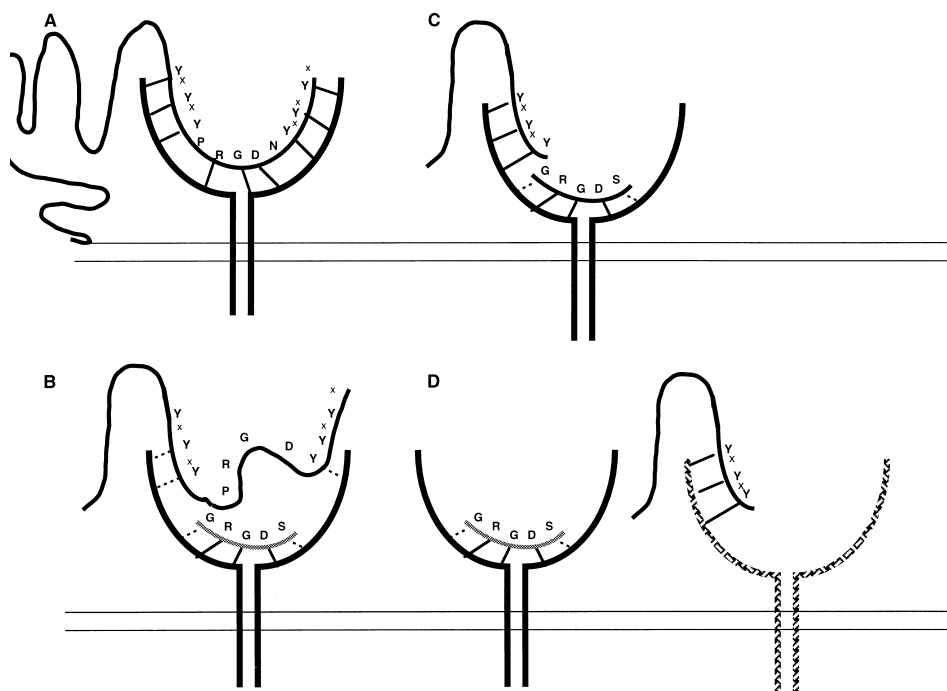


FIG. 8. Models of BSP-cell surface protein interactions. BSP contains conserved tyrosine-rich sequences that facilitate cell adhesion. Conserved tyrosines are denoted as (Y) and nonconserved amino acids are denoted as x. (A) In the first model, the conserved C-terminal BSP tyrosines interact with an integrin-like cell surface receptor(s) to facilitate cell attachment. (B) The ability of GRGDS to modulate the interaction of 258E–317Q BSP with the receptor may be due to steric hindrance. (C) However, 205S–281E lacking the RGD region would be expected to interact with the receptor in the presence of GRGDS. (D) Alternatively in a second model, BSP may interact with novel receptors and the observed effects of GRGDS may be due to down-stream biological effects of GRGDS upon the cell.

ondary structure reported earlier,⁽⁴⁴⁾ direct proof was until now unavailable. Of course the structure of this domain upon binding of its receptor or even when interacting with other portions of the BSP may be considerably different from the random coil presented here. Tyrosine sulfation may also confer a more rigid structure upon this domain. While several RGD-containing short peptides have been shown to contain stable loop conformations at the RGD site,^(45,46) most of the RGD-containing proteins reported in the past have also lacked a defined conformation at their RGD sites.^(47,48) Because the peaks were relatively strong, Fig. 4 also suggests that this domain is a monomer at ~10 mg/ml.

In summary, we have shown that natural BSP is a strong apatite-binding protein. At least a portion of this binding ability is encoded throughout a sizable stretch of the protein sequence itself. Furthermore, we have also demonstrated that BSP utilizes non-RGD tyrosine-rich sequences as well as its RGD sequence to mediate cell adhesion. NMR analysis of the integrin binding domain shows that at least the RGD domain is a random coil in solution. However, several questions remain. Results obtained from Mintz et al.⁽¹⁶⁾ and this study clearly demonstrate that the classic BSP RGD-encoded cell attachment domain can be separated from the BSP HA inhibitory domains through the action of an endogenous UMR-106-01 osteosarcoma protease. Moreover, the classic RGD cell attachment domain may be

separated from the non-RGD cell attachment domains described here. Several investigators have observed immunoreactive BSP species smaller than mature BSP in the serum of normal patients.^(49,50) Moreover, possibly similar low molecular weight BSP species are reported to increase with time during BMP-induced ectopic bone formation.⁽⁵¹⁾ To date, it is unknown if these species represent enzymatic fragments of mature BSP or mature BSP lacking specific post-translational modifications. However, it is tempting to speculate that these species participate directly in hydroxyapatite crystal modulation and/or cell interactions given the cell adhesive and HA modulatory activities of the human BSP recombinant fragments. Additional studies are underway to define BSP functions.

REFERENCES

1. Fisher LW, Whitson SW, Avioli LV, Termine JD 1983 Matrix sialoprotein of developing bone. *J Biol Chem* **258**:12723–12727.
2. Bianco P, Fisher LW, Young MF, Termine JD, Robey PG 1991 Expression of bone sialoprotein (BSP) in developing human tissues. *Calcif Tissue Int* **49**:421–426.
3. Chen J, Shapiro HS, Sodek J 1992 Development expression of bone sialoprotein mRNA in rat mineralized connective tissues. *J Bone Miner Res* **7**:987–997.
4. Macneil RL, Sheng N, Strayhorn C, Fisher LW, Somerman MJ

- 1994 Bone sialoprotein is localized to the root surface during cementogenesis. *J Bone Miner Res* **9**:1597–1606.
5. Bellahcene A, Merville MP, Castronovo V 1994 Expression of bone sialoprotein, a bone matrix protein, in human breast cancer. *Cancer Res* **54**:2823–28236.
6. Bellahcene A, Kroll M, Liebens F, Castronovo V 1996 Bone sialoprotein expression in primary human breast cancer is associated with bone metastases development. *J Bone Miner Res* **11**:665–670.
7. Ibaraki K, Termine JD, Whitson SW and Young MF 1992 Bone matrix mRNA expression in differentiating fetal bovine osteoblasts. *J Bone Miner Res* **7**:743–754.
8. Kasugai S, Todescan Jr R, Nagata T, Yao K-L, Butler WT, Sodek J 1991 Expression of bone matrix proteins associated with mineralized tissue formation by adult rat bone marrow cells in vitro: Inductive effects of dexamethasone on the osteoblastic phenotype. *J Cell Physiol* **147**:111–120.
9. Aubin JE, Gupta A, Zirnbibl R, Rossant J 1995 Bone sialoprotein knockout mice have bone abnormalities. *Bone* **17**:558.
10. Bianco P, Riminucci M, Silvestrini G, Bonucci E, Termine JD, Fisher LW, Robey PG 1993 Localization of bone sialoprotein (BSP) to Golgi and post-Golgi secretory structures in osteoblasts and to discrete sites in early bone matrix. *J Histochem Cytochem* **41**:193–203.
11. Hunter GK, Goldberg HA 1993 Nucleation of hydroxyapatite by bone sialoprotein. *Proc Natl Acad Sci USA* **90**:8562–8565.
12. Hunter GK, Goldberg HA 1994 Modulation of crystal formation by bone phosphoproteins: Role of glutamic acid-rich sequences in the nucleation of hydroxyapatite by bone sialoprotein. *Biochem J* **302**:175–179.
13. Somerman MJ, Fisher LW, Foster RA, Sauk JJ 1988 Human bone sialoprotein I and II enhance fibroblast attachment in vitro. *Calcif Tissue Int* **43**:50–53.
14. Helfrich MH, Nesbitt SA, Dorey EL, Horton MA 1992 Rat osteoclasts adhere to a wide range of RGD (Arg-Gly-Asp) peptide-containing proteins, including the bone sialoproteins and fibronectin, via a beta 3 integrin. *J Bone Miner Res* **7**:335–343.
15. Loeser RF 1993 Integrin-mediated attachment of articular chondrocytes to extracellular matrix proteins. *Arthritis Rheum* **36**:1103–1110.
16. Mintz KP, Grzesik WJ, Midura RJ, Robey PG, Termine JD, Fisher LW 1993 Purification and fragmentation of nondenatured bone sialoprotein: Evidence for a cryptic, RGD-resistant cell attachment domain. *J Bone Miner Res* **8**:985–995.
17. van Pluijm G, Kerr J, Lowik C, Robey P 1993 B1 and B3 integrin subunits are involved in adhesion of breast cancer cells to extracellular bone matrix. *J Bone Miner Res* **8** (Suppl 1):S136.
18. van der Pluijm G, Vloedgraven HJM, Ivanov B, Robey FA, Grzesik WJ, Robey PG, Papapoulos SE, Lowik CWGM 1996 Bone-sialoprotein are potent inhibitors of breast cancer cell adhesion to bone. *Cancer Res* **56**:1948–1955.
19. Oldberg A, Franzen A, Heinegard D 1988 The primary structure of a cell-binding bone sialoprotein. *J Biol Chem* **263**: 19430–19432.
20. Oldberg A, Franzen A, Heinegard D, Pierschbacher M, Ruoslahti E 1988 Identification of a bone sialoprotein receptor in osteosarcoma cells. *J Biol Chem* **263**:19433–19436.
21. Fisher LW, McBride OW, Termine JD, Young MF 1990 Human bone sialoprotein: Deduced protein sequence and chromosomal localization. *J Biol Chem* **265**:2347–2351.
22. Shapiro HS, Chen J, Wrana JL, Zhang Q, Blum M, Sodek J 1993 Characterization of porcine bone sialoprotein: Primary structure and cellular expression. *Matrix* **13**:431–440.
23. Young MF, Ibaraki K, Kerr JM, Lyu MS, Kozak CA 1994 Murine bone sialoprotein (BSP): cDNA cloning, mRNA expression, and genetic mapping. *Mamm Genome* **5**:108–111.
24. Yang R, Gotoh Y, Moore MA, Rafidi K, Gerstenfeld LC 1995 Characterization of an avian bone sialoprotein (BSP) cDNA: Comparisons to mammalian BSP and identification of conserved structural domains. *J Bone Miner Res* **10**:632–640.
25. Sasaguri K, Chen J 1996 Genebank accession number U65889.
26. Stubbs III JT, Eanes ED, Fisher, LW 1995 The use of native and recombinant fragments to delineate non-RGD cell attachment domains and mineral-binding domains of bone sialoprotein. *J Bone Miner Res* **10** (Suppl 1):S432.
27. Mintz KP, Midura RJ, Fisher LW 1994 Purification of bone sialoprotein from the medium of the rat osteoblast-like cell line UMR 106-01 BSP. *J Tissue Culture Meth* **16**:205–209.
28. Young MF, Kerr JM, Termine JD, Wewer UM, Wang MG, McBride OW, Fisher LW 1990 cDNA cloning, mRNA distribution and heterogeneity, chromosomal location, and RFLP analysis of human osteopontin (OPN). *Genomics* **7**:491–502.
29. Stubbs III JT 1996 The generation and use of recombinant bone sialoprotein and osteopontin for hydroxyapatite studies. *Connect Tissue Res* **35**:393–399.
30. Midura RJ, McQuillan DJ, Benham KJ, Fisher LW, Hascall VC 1990 A rat osteogenic cell line (UMR 106-01) synthesizes a highly sulfated form of bone sialoprotein. *J Biol Chem* **265**:5285–5291.
31. Scatchard G 1949 The attraction of proteins for small molecules and ions. *Ann NY Acad Sci* **51**:660–672.
32. Boskey AL, Maresca M, Ullrich W, Doty SB, Butler WT, Prince CW 1993 Osteopontin hydroxyapatite interactions in vitro inhibition of hydroxyapatite formation and growth in a gelatin-gel. *Bone Miner* **22**:147–159.
33. Moreno EC, Kresak M, Hay DI 1982 Adsorption thermodynamics of acidic proline-rich human salivary proteins onto calcium apatites. *J Biol Chem* **257**:2981–2989.
34. Green MR, Pastewka JV, Peacock AC 1973 Differential staining of phosphoproteins on polyacrylamide gels with a cationic carbocyanine dye. *Anal Biochem* **56**:43–51.
35. Hu DD, Hoyer JR, Smith JW 1995 Ca²⁺ suppresses cell adhesion to osteopontin by attenuating binding affinity for integrin $\alpha_5\beta_3$. *J Biol Chem* **270**:9917–9925.
36. Andrieux A, Hudry-Clergeon G, Ryckewaert JJ, Chapel A, Ginsberg MH, Plow EF, Marguerie G 1989 Amino acid sequences in fibrinogen mediating its interaction with its platelet receptor, GPIIb/IIIa. *J Biol Chem* **264**:9258–9265.
37. Ginsberg M, Pierschbacher MD, Ruoslahti E, Marguerie G, Plow E 1985 Inhibition of fibronectin binding to platelets by proteolytic fragments and synthetic peptides which support fibroblast adhesion. *J Biol Chem* **260**:3931–3936.
38. Romberg RW, Werness PG, Riggs BL, Mann KG 1986 Inhibition of hydroxyapatite crystal growth by bone-specific and other calcium-binding proteins. *Biochemistry* **25**:1176–1180.
39. Franzen A, Heinegard D 1985 Isolation and characterization of two sialoproteins present only in bone calcified matrix. *Biochem J* **232**:715–724.
40. Heinegard D, Hultenby K, Oldberg A, Reinholt F, Wendel M 1989 Macromolecules in bone matrix. *Connect Tissue Res* **21**:3–14.
41. Ecarot-Charrier B, Bouchard F, Delloye C 1989 Bone sialoprotein II synthesized by cultured osteoblasts contains tyrosine sulfate. *J Biol Chem* **264**:20049–20053.
42. Kinne RW, Fisher LW 1987 Keratan sulfate proteoglycan in rabbit compact bone is bone sialoprotein II. *J Biol Chem* **262**:10206–10211.
43. Mechref Y, El Rassi Z 1994 Capillary electrophoresis of carboxylated carbohydrates I. Selective precolumn derivatization

- of gangliosides with UV absorbing and fluorescent tags. *Electrophoresis* **15**:627–634.
44. Fisher LW 1992 Structure/Function studies of the sialoproteins and proteoglycans of bone. In: *Chemistry and Biology of Mineralized Tissues*. Slavkin H, Price P (eds.) Elsevier Publishers B.V., New York, NY, U.S.A. pp. 177–186.
 45. Johnson WC, Pagano TG, Basson CT, Madri JA, Gooley P, Armitage IM 1993 RGD oligopeptide assume a type II b-turn in solution. *Biochemistry* **32**:268–273.
 46. Krezel AM, Wagner G, Seymour-Ulmer J, Lazarus RA 1994 Decorsin: Structure of the RGD protein decorsin: conserved motif and distinct function in leech proteins that affect blood clotting. *Science* **264**:1944–1947.
 47. Adler M, Wagner G 1992 Kistrin, Sequential ¹H NMR assignments of kistrin, a potent platelet aggregation inhibitor and glycoprotein IIb-IIIa antagonist. *Biochemistry* **31**:1031–1039.
 48. Dickinson CD, Veerapandian B, Dai XP, Hamlin RC, Xuong NH, Ruoslahti E, Ely KR 1994 Crystal structure of the tenth type III cell adhesion module of human fibronectin. *J Mol Biol* **236**:1079–1092.
 49. Mansson B, Carey D, Alini M, Ionescu M, Rosenberg LC, Poole AR, Heinegard D, Saxne T 1995 Cartilage and bone metabolism in rheumatoid arthritis: Differences between rapid and slow progression of disease identified by serum markers of cartilage metabolism. *J Clin Invest* **95**:1071–1077.
 50. Chenu C, Delmas PD 1992 Platelets contribute to circulating levels of bone sialoprotein in human. *J Bone Miner Res* **7**:47–54.
 51. Kobayashi D, Takita H, Mizuno M, Totsuka Y, Kuboki Y 1996 Time-dependent expression of bone sialoprotein fragments in osteogenesis induced by bone morphogenetic protein. *J Biochem* **119**:475–481.

Address reprint requests to:

John T. Stubbs III
BRB, NIDR, National Institutes of Health
Room 106, Building 30
Bethesda, MD 20892 U.S.A.

Received in original form December 19, 1996; in revised form March 21, 1997; accepted March 31, 1997.